Author/s:
Li, J;Ma, HZ;Reid, GE;Edwards, AJ;Hong, Y;White, JM;Mulder, RJ;O'Hair, RAJ

Title:
Synthesis and X-Ray Crystallographic Characterisation of Frustum-Shaped Ligated [Cu18H16(DPPE)6]2+ and [Cu16H14(DPPA)6]2+ Nanoclusters and Studies on Their H2 Evolution Reactions

Date:
2018-02-09

Citation:
Li, J., Ma, H. Z., Reid, G. E., Edwards, A. J., Hong, Y., White, J. M., Mulder, R. J. & O'Hair, R. A. J. (2018). Synthesis and X-Ray Crystallographic Characterisation of Frustum-Shaped Ligated [Cu18H16(DPPE)6]2+ and [Cu16H14(DPPA)6]2+ Nanoclusters and Studies on Their H2 Evolution Reactions. Chemistry A European Journal, 24 (9), pp.2070-2074. https://doi.org/10.1002/chem.201705448.

Persistent Link:
https://hdl.handle.net/11343/283514

Title: Synthesis and X-ray Crystallographic Characterisation of Frustum-Shaped Ligated [Cu18H16(DPPE)6]2+ and [Cu16H14(DPPA)6]2+ Nanoclusters and Studies on their H2 Evolution Reactions

Authors: Jiaye Li; Howard Zihao Ma; Gavin Reid; Alison Edwards; Yuning Hong; Jonathan White; Roger Mulder; Richard A J O'Hair, PhD DSc

To be cited as: 10.1002/chem.201705448

Link to VoR: https://doi.org/10.1002/chem.201705448

Synthesis and X-ray Crystallographic Characterisation of Frustum-Shaped Ligated $[Cu_{18}H_{16}(DPPE)_6]^{2+}$ and $[Cu_{16}H_{14}(DPPA)_6]^{2+}$ Nanoclusters and Studies on their H_2 Evolution Reactions

Jiaye Li,*[a] Howard Z. Ma,[a] Gavin E. Reid,[a,b] Alison J. Edwards,[c] Yuning Hong,[a] Jonathan M. White,[a] Roger J. Mulder,[d] and Richard A. J. O'Hair*[a]

Abstract: We report new structural motifs for Cu nanoclusters that conceptually represent seed crystals for large face-centred cubic (FCC) crystal growth. Kinetically controlled syntheses, high resolution mass spectrometry experiments for determination of the dication formulae and crystallographic characterisation were carried out for $[Cu_{18}H_{16}(DPPE)_6][BF_4][Cl]$ (DPPE = bis(diphenylphosphino)ethane) and $[Cu_{16}H_{14}(DPPA)_6][(BF_4)_2]$ (DPPA = bis(diphenylphosphino)amine) polyhydrido nanoclusters, which feature the unprecedented bifrustum and frustum metal-core architecture in metal nanoclusters. The Cu_{18} nanocluster contains two Cu_9 frustum cupolae and the Cu_{16} nanocluster has one Cu_9 frustum cupola and a Cu_7 distorted hexagonal-shape base. Gas-phase experiments revealed that both $Cu_{18}H_{16}$ and $Cu_{16}H_{14}$ cores can spontaneously release H_2 upon removal of one bisphosphine capping ligand.

Although it is currently possible to control the sizes and shapes of nanoparticles, the manipulation of individual atoms to construct nano-sized materials with varied properties remains elusive. Thus, atomically precise nanoparticles (NPs) or nanoclusters (NCs) have emerged as an important new class of nanomaterials. Due to their well-defined numbers of atoms and ligands, confined sizes and precise structures, they exhibit molecular-like properties, which makes them attractive for single-site catalysis,[1] switchable subnano-magnetism,[2] chemical sensing,[3] biological labelling and biomedical applications,[4] in addition to light-emitting devices.[5] In particular, understanding the metal-hydrogen interaction from a molecular perspective will provide insights into the utilisation of atomically precise NPs or NCs as potential energy materials and as catalysts for the transformation of organic substrates.

There are a number of structurally characterised polyhydrido copper[6] and silver NCs,[6i, 7] where the rare kernel examples are Cu(0) NCs [6f] or chiral Cu NCs.[6g] The synthesis of unknown metal kernels can provide insight into the growth mechanism of large nanoparticles.[8] Face-centred cubic (FCC) is a common structural motif in many examples of single or twinned crystalline Au NCs[9] and Ag FCC nanocrystals can grow from the Au seed nanocrystals that have triangular-bifrustum structures.[10] The organisation of the copper kernel in polyhydrido Cu NCs normally adopt zonohedron[11] and other polyhedra such as dodecahedron,[12] tetrahedron,[13] rhombicuboctahedron,[14] orthobicupola,[6d,15] distorted cuboctahedron[6g] and octahedron.[16] The FCC kernel motif for Cu NCs was unknown until Chakrahari *et al.* reported a Cu_{13} cuboctahedron, which occurs in the FCC structure of copper bulk metal.[17] However, there are still no such noble metal NCs that have shown triangular bifrustum motifs, which are the key to growing FCC type large nanoparticles. Herein, we report the first and smallest possible triangular bifrustum structure of Cu NCs. Four new cationic $[Cu_{18}H_{16}(L)_6]^{2+}$ ($\mathbf{1_H}^{2+}$), $[Cu_{18}D_{16}(L)_6]^{2+}$($\mathbf{1_D}^{2+}$), $[Cu_{16}H_{14}(L^*)_6]^{2+}$ ($\mathbf{2_H}^{2+}$) and $[Cu_{16}D_{14}(L^*)_6]^{2+}$ ($\mathbf{2_D}^{2+}$) nanoclusters, stabilised by bis(diphenylphosphino)ethane, DPPE (L) or bis(diphenylphosphino)amine (L*) were synthesised. $\mathbf{1_H}^{2+}$ and $\mathbf{2_H}^{2+}$ were characterised by X-ray crystallography, while high-resolution tandem mass spectrometry experiments were used to study hydrogen evolution from the nanocluster dications.

The nanoclusters of $[Cu_{18}H_{16}(DPPE)_6][BF_4][Cl]$ ($\mathbf{1_H}$) and $[Cu_{16}H_{14}(DPPA)_6][(BF_4)_2]$ ($\mathbf{2_H}$) were synthesised by the reactions of $Cu(MeCN)_4BF_4$ with sub-stoichiometric quantities of ligands and slight excess of borohydride salts (for full details, see Supporting Information).[6h] The related deuterated nanoclusters ($\mathbf{1_D}$ and $\mathbf{2_D}$) were obtained similarly using borodeuteride salts. The isotope patterns (Supporting Information Figure S1) and accurate masses from positive ion mode Electrospray Ionisation - Ultra-High Resolution Accurate Mass Spectrometry (ESI-UHRAMS) experiments helped establish the formulae of $\mathbf{1_H}^{2+}$ as $[Cu_{18}H_{16}(DPPE)_6]^{2+}$ (*m/z* 1774.8338 (expt)/1774.8322 (calc)) and $\mathbf{2_H}^{2+}$ as $[Cu_{16}H_{14}(DPPA)_6]^{2+}$ (*m/z* 1670.8301 (expt)/1670.8340 (calc)). The number of hydrides were "counted" by comparing the deuterated analogues $\mathbf{1_D}^{2+}$ and $\mathbf{2_D}^{2+}$ to $\mathbf{1_H}^{2+}$ and $\mathbf{2_H}^{2+}$. $\mathbf{1_D}^{2+}$ (expt/calc: 1782.8789/1782.8825), is 8 *m/z* heavier, indicating the presence of 16 hydrides in $\mathbf{1_H}^{2+}$. A similar analysis of $\mathbf{2_D}^{2+}$ (*m/z* 1677.8723/1677.8780) revealed the presence of 14 hydrides in $\mathbf{2_H}^{2+}$.

The nanoclusters $\mathbf{1_H}$ and $\mathbf{2_H}$ were crystallised by slow diffusion of hexane into dichloromethane (DCM) solutions with $\mathbf{1_H}$ or $\mathbf{2_H}$. Structural characterisation of $\mathbf{1_H}$ and $\mathbf{2_H}$ with X-ray single-crystal diffraction was performed (Supporting Information Figures S2-S4, Tables S1-S4) to reveal the new core architectures and ligand coordination motifs in the Cu nanoclusters (Figure 1).[18] The nanocluster $\mathbf{1_H}$ crystallises in space group $P2_1/n$ with two enantiomeric pairs of $\mathbf{1_H}^{2+}$ (Figure 1), four BF_4 and four chloride counterions per unit cell. There are two ways of considering the structure of the cationic component of $\mathbf{1_H}$: (i) As a Cu_{18} core surrounded by six DPPE ligands, which divide the Cu atoms into two groups. The first group consists of 12 Cu "staple" atoms (represented as the orange balls in Figure 1 (a)), bonded to the P atoms of DPPE. In contrast, the central Cu_6 core forms no direct bonds with the DPPE ligands and has a distorted octahedral geometry. The average distance of the two long edges in the Cu_6 core is 3.16 Å, much longer than the average contact distance (2.73 Å) of the short edges in the octahedral structure and other Cu-Cu contact

[a] Dr. J. Li*, Mr. H. Z. Ma, Prof. G. E. Reid, Dr. Y. Hong, Prof. J. M. White, and Prof. R. A. J. O'Hair*
School of Chemistry and Bio21 Molecular Science and Biotechnology Institute
University of Melbourne
30 Flemington Rd, Parkville, Victoria 3010, Australia
E-mail: rohair@unimelb.edu.au & jiaye.li@unimelb.edu.au
[b] Prof. G. E. Reid
Department of Biochemistry and Molecular Biology
University of Melbourne
30 Flemington Rd, Parkville, Victoria 3010, Australia
[c] Dr. A. J. Edwards
Australian Centre for Neutron Scattering, Australian Nuclear Science and Technology Organisation
New Illawarra Road, Lucas Heights, NSW 2234, Australia
[d] Dr. R. J. Mulder
CSIRO Manufacturing
Research Way, Clayton, Victoria 3168, Australia

distances (d_{Cu-Cu} = 2.63 – 2.68 Å) in the distorted octahedral core of $H_6Cu_6[P(p\text{-tolyl})_3]_6$.[19] Together these two groups of Cu atoms form the Cu_6@(Cu_{12}DPPE) kernel@staple motif. Similar octahedron kernel building blocks were also reported recently in the Au_8 unit of Au_{18} nanoclusters[20] and in the anti-prism $[Cu_8H]^{7+}$ unit in $[Cu_{18}H_{17}(TPP)_{10}]^+$, TPP = triphenylphosphine.[6f] (ii) The Cu_{18} core can alternatively be described as an elongated and distorted triangular bifrustum construct. Although the bifrustum shape is commonly observed in large nanocrystals, such as the triangular bifrustum Ag nanolayer shell structure,[21] as far as we are aware, this represents a new polyhedral core motif in nanoclusters (other core packing motifs in nanoclusters include tetrahedral,[10] cuboctahedral,[6g] rhombicuboctahedral,[6g] hexagonal close-pack,[20, 22] decahedral,[23] icosahedral,[6f, 24] face-centred cubic[25] and body-centred cubic[26]). A pair of Cu_6 triangular cupolae lie with their approximate 3-fold axes coincident and long trapezoidal edges forming an equatorial C_6 band, which enclose the non-phosphine ligated Cu_6 distorted octahedron, the vertices of which lie at the approximate midpoints of the long cupola edges to form the overall core structure, which is an elongated triangular bifrustum. The Cu-Cu links between the opposing cupolae (and the configuration of the bidentate phosphine ligands) are disposed in a manner which results in a molecular chirality of the screw (or propeller) kind.[6g] The compound crystallises as a racemate. In a related manner, the Cu_{16} compound is also chiral. The edge distances of Cu-Cu contacts in the Cu_9 cupola range from 2.3837(11) Å to 2.8179(15) Å, comparable to Cu-Cu distances in other polynuclear copper hydride complexes.[6h]

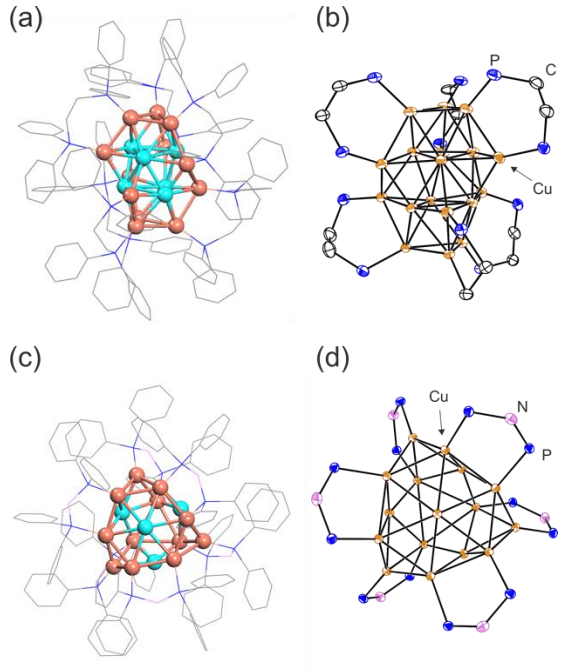

Figure 1. (a) Complete structure of the cationic component of $\mathbf{1_H}$. (b) Ortep-3 structure of Cu_{18}^{2+} core with partially shown ligand (25% ellipsoid probability). (c) Complete structure of the cationic component of $\mathbf{2_H}$. (d) Ortep-3 structure of Cu_{16}^{2+} core with partially shown ligand (25% ellipsoid probability). Anions and hydrogens are omitted for clarity. Phenyl groups were omitted in (b) and (d) for clarity. Colour indications, orange: staple Cu, cyan: kernel Cu, blue: phosphorous, pink: nitrogen, grey: carbon. Ligands are displayed in lines.

The nanocluster $\mathbf{2_H}$ crystallised in space group Pa-3. Only a limited amount of crystals of $\mathbf{2_H}$ could be manually picked up. This is likely due to the elusive nature of the $\mathbf{2_H}^{2+}$ core, which had dissociated to form black metal solids deposited in the crystallisation tube. Figure 1 (c) and (d) illustrate the cationic components ($\mathbf{2_H}^{2+}$) of $\mathbf{2_H}$. Unlike $\mathbf{1_H}^{2+}$, $\mathbf{2_H}^{2+}$ cannot be represented by the kernel@staple model, due to the non-interacting long kernel Cu-Cu distances (> 3.1 Å, highlighted in cyan in Figure 1 (c)).[27] Instead the core motif of $\mathbf{2_H}^{2+}$ can best be described as stacking a triangular Cu_9 frustum onto a distorted hexagonal Cu_7 base (Figure 2 (c) and (d)). The Cu_9 frustum motifs in $\mathbf{1_H}$ and $\mathbf{2_H}$ appear to be new core architectures for size-precise noble metal nanoclusters.

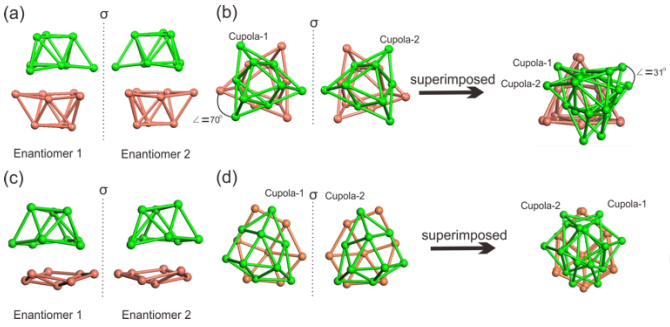

Figure 2. (a) The side view of the racemic Cu_{18} kernels (top cupola: green; bottom cupola: orange), divided by mirror symmetry (σ); (b) The top view of two racemic Cu_{18} kernels and the superimposed bottom cupolas (orange). (c) The side view of the racemic Cu_{16} kernels (top cupola: green; bottom cupola: orange), divided by mirror symmetry (σ); (d) The top view of two racemic Cu_{16} kernels and the superimposed bottom cupolas (orange). The drawings of bonds between top and bottom cupolae are not shown.

In the structure of each Cu_9 frustum cupola of $\mathbf{1_H}$ and $\mathbf{2_H}$, three bidentate diphosphine ligands are similarly arranged in a connective pattern on the side edges of the cupola. In $\mathbf{2_H}$, the Cu_7 base is connected by three DPPA ligands forming the (μ, μ-Cu_2DPPA)$_3$ motif. However, when the middle backbone unit in the ligands is changed from "NH" in DPPA to "CH_2CH_2" in DPPE, a dramatic change in the core construct and composition occurs, highlighting the importance of the ligand on the kernel structures of nanoclusters.[28] Indeed, similar ligand effects have been noted in forming $[Ag_{25}H_{22}(DPPE)_8]^{3+}$ and $[Ag_{18}H_{16}(TPP)_{10}]^{2+}$ under similar preparative conditions.[7a] The calculated ratio of Cu atoms to ligands in $\mathbf{1_H}$ is 3, higher than those in other polynuclear Cu nanoclusters such as $[Cu_3H(dcpm)_3]^{2+}$,[29] $[CuH(PPh_3)]_6$,[30] $[Cu_3H_3(dppbz)_3]$,[30] $[Cu_6H_6(p\text{-tolyl})_3]_6$,[19] $[Cu_{25}H_{22}(PPh_3)_{12}]^+$,[6f] and $[Cu_{18}H_{17}(PPh_3)_{10}]^+$.[6f] This suggests particular stability of the Cu_{18} core, which is investigated by MS below. Neutron single-crystal diffraction data[31] for $\mathbf{1_H}$ have been collected, but to date, no satisfactory indexing of the Laue images has been achieved.

NMR experiments were attempted to examine the compositions of these clusters in solution and to attempt to define the chemical environments of the coordinated hydrides. Since $\mathbf{2_H}$ was only isolated in a yield of ~2%, it was not possible to gather sufficient numbers of crystals for NMR experiments. Although every effort was made in manually sorting and collecting crystals of $\mathbf{1_H}$ for NMR analysis, it is acknowledged that the NMR sample may contain impurities from other crystalline material present in the crystallisation tube. The ^{1}H spectrum of $\mathbf{1_H}$ is consistent with the proposed formulation of $[Cu_{18}H_{16}(DPPE)_6]^{2+}$, where peaks in the δ 6.2 – 8.5 ppm region correspond to the phenyl protons of the DPPE ligand, while those in the δ 1.5 ~ 2.5 region arise from the coordinated hydrides and the methylene protons of the DPPE ligand (Figures S5 and S6) This is evidenced by the integration of proton signals to give 40 protons at δ 1.5 ~ 2.5 region and 120 protons at δ 6.2 – 8.5. The ^{13}C spectrum of $\mathbf{1_H}$ (Figure S7) exhibits resonances of *C*H$_2$ (δ 31 ppm) and Ph*C* (δ 125 ~ 135 ppm) associated with the DPPE ligands. The ^{31}P NMR spectrum (Figure S8a) at 25 °C gives resonances related to the P atoms of DPPE

ligands at ~ δ - 7 to -10 and -11 ppm. On cooling to -15 °C, the ^{1}H NMR spectrum remains essentially unchanged (Figure S6), while in the ^{31}P NMR spectrum the broad set of peaks in the - 7 to -10 ppm range become one main sharp peak at ~ -8.5 ppm (Figure S8b). This suggests dynamic, conformational processes involving the coordinated DPPE ligands which affects the resonances of the coordinated P atoms more than those of the H atoms of the freely rotating phenyl groups.

To better understand the processes leading to the formation of **1** and **2**, a series of "*in-situ*" experiments were carried out. In the first of these, ESI-UHRAMS (Figure S9) was used to examine the reaction solution mixtures of $\mathbf{1_D}^{2+}$ and $\mathbf{2_D}^{2+}$. $\mathbf{1_D}^{2+}$ is the main nanocluster observed. In contrast, the *in-situ* UHRAMS spectrum of $\mathbf{2_D}^{2+}$ is more complex, with other abundant nanoclusters $[Cu_3(BD_4)(D)(DPPA)]^{+}$ [6h] and $[Cu_6D_4(DPPA)_4]^{2+}$ also being observed. Importantly, we see no evidence for $[Cu_{18}D_{16}(DPPA)_6]^{2+}$, highlighting the key role of the ligand on the growth of these nanoclusters. We next compared the ^{1}H NMR spectra for the *in-situ* reactions with $NaBH_4$ versus $NaBD_4$ for **1** (Figure S10) and **2** (Figure S11). The former gives a series of peaks in 1.5 – 2.5 ppm range, consistent with the spectrum of the bulk $\mathbf{1_H}$ sample. The latter, gives a complex series of peaks at 0.5 – 1.5 ppm and 2.1 – 2.4 ppm, probably falling in the hydride or borohydride regions.[6h] The ^{2}H NMR spectra were collected for related *in-situ* experiments for $\mathbf{1_D}$ (Figure S12) and $\mathbf{2_D}$ (Figure S13). The ^{2}H resonances can be found in the 1.5 – 2.5 ppm range for $\mathbf{1_D}$ and in the 0.5 - 1.15 ppm and 2.1 – 2.4 ppm ranges for $\mathbf{2_D}$, which are in agreement with the hydride ranges (Figures S11 and S12). The ^{31}P NMR spectrum of $\mathbf{1_D}$ (Figure S14) shows resonances in the 15 to -15 ppm range and there is significant peak broadening in the 15 to -0.5 ppm range, which is consistent with the fact that we are not dealing with a pure sample. Due to the presence of other clusters, the assignment of specific hydride/deuteride resonances to $\mathbf{2_H}$ and $\mathbf{2_D}$ is impossible. The significant residual peaks in the electron density of the reported crystal structures are located on the external surfaces of the core and lie in positions that are consistent with the resonances reported here and with hydride/deuteride signals for copper hydride cluster compounds for which single-crystal neutron diffraction and proton and deuterium NMR are reported.[6g,11,32]

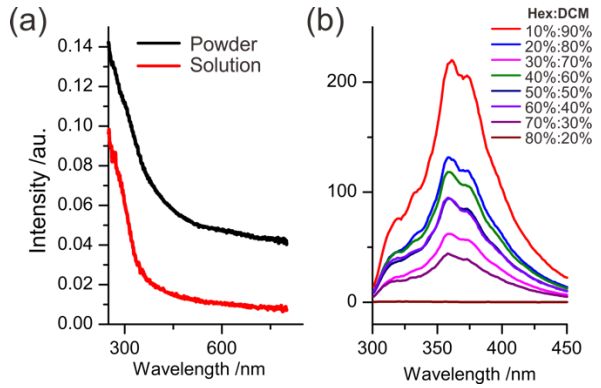

Figure 3. (a) UV-vis absorption spectra of $\mathbf{1_H}$ in an acetonitrile solution (red) and as solid (black); (b) Emission spectra of $\mathbf{1_H}$ in hexane (Hex) and dichloromethane (DCM) mixture solutions with the relative fractions of Hex to DCM ranging from 1:9 to 8:2 (v/v). Excitation wavelength: 280 nm.

Powders of $\mathbf{1_H}$ have the same UV absorption and emission spectra as in solution (Figure 3), suggesting that the structure of the Cu_{18} core stays intact in the acetonitrile solution. The absorption band increases monotonically and exponentially from 360 nm to 250 nm, representing a common absorption band of Cu nanoclusters in solution,[33] and is attributed to the d→sp interband transition. No absorption band is observed at 500 - 700 nm, which is a signature absorption feature for the intraband HOMO-LUMO transition (sp → sp) in Au nanoclusters.[9, 20a] To provide further information on cluster integrity in solutions, we studied the emission spectra of $\mathbf{1_H}$ in the solvent mixtures of DCM as good solvent for $\mathbf{1_H}$ and hexane as poor solvent with different volume proportions. Maintaining the analyte concentration constant, the proportion of hexane was increased from 10% to 90%, where the emission intensity decreased consistently. This supports the view that the concentrated $\mathbf{1_H}$ nanoclusters in hexane-rich solutions caused the fast collision of nanoclusters *via* a dynamic quenching effect.[34] Thus $\mathbf{1_H}$ retains its core integrity in solution, consistent with the ^{1}H NMR spectrum discussed above (Figures S5 and S6).

Polyhydrido nanoclusters are potential catalysts for hydrogen evolution reactions (HER), with possible applications in fuel-cell batteries.[9] The recyclable use of nanoclusters in constant energy production requires that the integrity of the metal kernel in nanoclusters be preserved after HER.[8, 35] As indicated above, the core integrity of $\mathbf{1_H}$ remained stable in solution, in the gas phase under ESI-MS conditions and as solid under ambient conditions. We investigated the HER process of $\mathbf{1_H}$ and $\mathbf{2_H}$ via Higher Energy Collision Dissociation - tandem mass spectrometry (HCD-MS/MS) experiments (Figure 4). Initial removal of one ligand from $\mathbf{1_H}^{2+}$ and $\mathbf{2_H}^{2+}$ triggers the subsequent and spontaneous HER from the product ions $[Cu_{18}H_{16}(L)_5]^{2+}$ (L = DPPE, *m/z* 1569.7642 (expt)/1569.7648 (calc)) and $[Cu_{16}H_{14}(L^*)_5]^{2+}$ (L^* = DPPA, *m/z* 1665.8312 (expt)/ 1665.8358 (calc)) to form a series of new cluster ions, which can be written as $[Cu_{18}H_x(L)_5]^{2+}$ (where x = even integers between 0 and 16, Figure 4) and $[Cu_{16}H_x(L^*)_5]^{2+}$ (where x = even integers between 0 and 14). When x = 0, the products are assigned as $[Cu_{18}(L)_5]^{2+}$ (*m/z* 1561.7052 (expt)/1561.7042 (calc)) and $[Cu_{16}(L^*)_5]^{2+}$ (*m/z* 1466.2205 (expt)/ 1466.2236 (calc)), which indicates the complete removal of hydrides to form rare examples of mixed-valence $Cu_{18}^{0/+}$ and $Cu_{16}^{0/+}$ nanoclusters.[6f, 36]

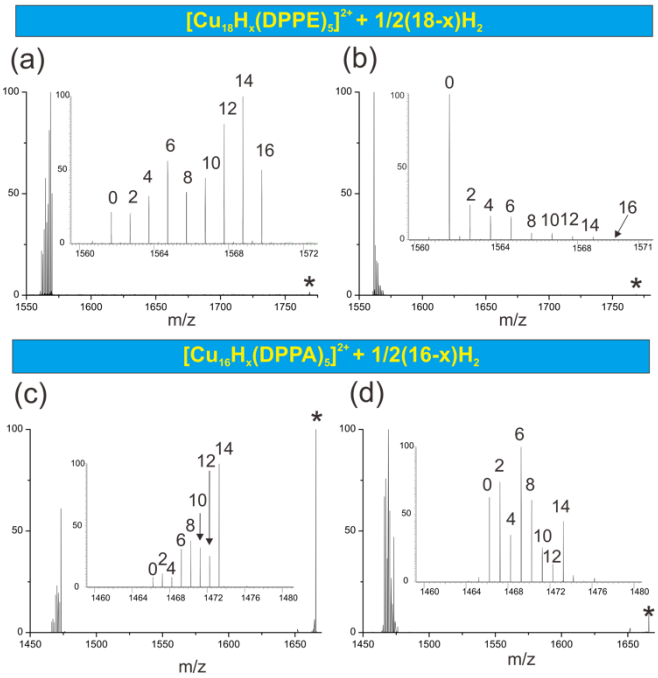

Figure 4. HCD-MS/MS liberation of H_2 from $\mathbf{1_H}^{2+}$ and $\mathbf{2_H}^{2+}$ and the formation of $[Cu_{18}(DPPE)_5]^{2+}$ (a, b) and $[Cu_{16}(DPPA)_5]^{2+}$ (c, d). (a) E_{HCD} = 8%, (b) E_{HCD} = 10%, (c) E_{HCD} = 9% and (d) E_{HCD} = 11%. Insets show an expanded region of the spectrum for the $[Cu_{18}Hx(DPPE)_5]^{2+}$ or $[Cu_{16}Hx(DPPA)_5]^{2+}$ product ions, x values are indicated in the insets.

To further examine the HER process, the HCD-MS/MS fragmentation reactions of the deuterated analogues $\mathbf{1_D}^{2+}$ and $\mathbf{2_D}^{2+}$ were examined (Figure S15). $\mathbf{1_D}^{2+}$ (*m/z* 1776.8762 (expt)/1776.8846 (calc)) underwent facile deligation to form $[Cu_{18}D_{16}(L)_5]^{2+}$ (*m/z* expt/calc 1577.8188/1577.8180) as the main product ion. $[Cu_{18}D_{16}(L)_5]^{2+}$ underwent facile D_2, HD, D and H loss channels to produce $[Cu_{18}D_{16-x}(L)_5]^{2+}$, $[Cu_{18}D_{16-x}(L)_5\text{-H}]^{2+}$, $[Cu_{18}D_{16-x}(L)_5\text{-D}]^{2+}$ and $[Cu_{18}D_{16-x}(L)_5\text{-HD}]^{2+}$. The observation of HD losses highlights that release of hydrogen is a complex process that involves H/D scrambling with the bisphosphine capping ligands. The channels to yield $[Cu_{18}D_{16-x}(L)_5]^{2+}$ and $[Cu_{18}D_{16-x}(L)_5\text{-HD}]^{2+}$ accounted for the main hydride-loss pathways. The complete D-loss from $[Cu_{18}D_{16}(L)_5]^{2+}$ generated the product ion $[Cu_{18}(L)_5]^{2+}$, also obtained from the complete hydride-loss of $[Cu_{18}H_{16}(L)_5]^{2+}$. Similarly, $[Cu_{16}D_{14}(L^*)_5]^{2+}$ underwent complete D-loss to yield $[Cu_{16}(L^*)_5]^{2+}$ under HCD conditions.

Given $\mathbf{1_H}^{2+}$ readily loses H_2 in the gas phase while maintaining Cu_{18} core integrity, we next used variable temperature ^{1}H NMR to examine the liberation of H_2 from a solution of $\mathbf{1_H}$ in $CDCl_3$, which was heated to 55 °C. Although the complete release of H_2 (δ 4.62 ppm) with concurrent disappearance of hydride peaks from δ 1.5 ~ 2.5 region was observed within minutes (Figure S16), changes in the chemical shifts of the DPPE ligands suggested that the core of $\mathbf{1_H}$ underwent decomposition. Similar HER from polyhydrido Cu nanoclusters have been observed before *via* treatments such as heating, acidification or solar radiation.[6d, 6e, 37]

In conclusion, nanoclusters that contain Cu_{18} and Cu_{16} chiral cores have been synthesised and crystallographically characterised. The cationic components of $\mathbf{1_H}$ and $\mathbf{2_H}$ are new, non-Johnson, polyhedral forms in noble metal nanocluster core aggregates. HCD-MS/MS experiments indicated the spontaneous H_2/D_2 production and ligand assisted scrambling reactions in mono-deligated $\mathbf{1_H}$ and $\mathbf{1_D}$.

Acknowledgements

R.A.J.O. acknowledges funding from the Australian Research Council (project number DP150101388). J. Li, A. J. Edwards, J. M. White and R.A.J.O acknowledge funding from the Australian Nuclear Science and Technology Organisation (project number 5579). G.E.R. acknowledges funding from the Australian Research Council (LE160100015).

Conflict of interest

The authors declare no conflict of interest.

Keywords: copper hydrides · coinage metal nanoclusters · X-ray crystallography · bifrustum structure · hydrogen release

[1] (a) E. C. Tyo, S. Vajda, *Nat. Nanotechnol.* **2015**, *10,* 577-588; (b) I. Chakraborty, T. Pradeep, *Chem. Rev.,* **2017**, *117,* 8208–8271; (c) A. J. Jordan, G. Lalic, J. P. Sadighi, Chem. Rev. **2016**, *116*, 8318-8372; (d) A. Zavras, G. N. Khairallah, M. Krstić, M. Girod, S. Daly, R. Antoine, P. Maitre, R. J. Mulder, S.-A. Alexander, V. Bonačić-Koutecký, P. Dugourd, R. A. J. O'Hair, *Nature Commun*. **2016**, *7*, 11746; (e) A. Zavras, M. Krstić, P. Dugourd, V. Bonačić-Koutecký, R. A. J. O'Hair, *ChemCatChem*, **2017**, *9,* 1298–1302.

[2] M. Zhu, C. M. Aikens, M. P. Hendrich, R. Gupta, H. Qian, G. C. Schatz, R. Jin, *J. Am. Chem. Soc.* **2009**, *131,* 2490-2492.

[3] L. Li, H. Liu, Y. Shen, J. Zhang, J.-J. Zhu, *Anal. Chem.* **2011**, *83,* 661-665.

[4] Z. Luo, K. Zheng, J. Xie, *Chem. Commun.* **2014**, *50,* 5143-5155.

[5] Z. Wu, R. Jin, *Nano Lett.* **2010**, *10,* 2568-2573.

[6] (a) S. A. Bezman, M. R. Churchill, J. A. Osborn, J. Wormald, *J. Am. Chem. Soc.* **1971**, *93,* 2063-2065; (b) T. H. Lemmen, K. Folting, J. C. Huffman, K. G. Caulton, *J. Am. Chem. Soc.* **1985**, *107,* 7774-7775; (c) C. Liu, B. Sarkar, Y.-J. Huang, P.-K. Liao, J.-C. Wang, J.-Y. Saillard, S. Kahlal, *J. Am. Chem. Soc.* **2009**, *131,* 11222-11233; (d) R. S. Dhayal, J.-H. Liao, Y.-R. Lin, P.-K. Liao, S. Kahlal, J.-Y. Saillard, C. Liu, *J. Am. Chem. Soc.* **2013**, *135,* 4704-4707; (e) A. J. Edwards, R. S. Dhayal, P. K. Liao, J. H. Liao, M. H. Chiang, R. O. Piltz, S. Kahlal, J. Y. Saillard, C. Liu, *Angew. Chem. Int. Ed.* **2014**, *126,* 7342-7346; (f) T.-A. D. Nguyen, Z. R. Jones, B. R. Goldsmith, W. R. Buratto, G. Wu, S. L. Scott, T. W. Hayton, *J. Am. Chem. Soc.* **2015**, *137,* 13319-13324; (g) R. S. Dhayal, J. H. Liao, X. Wang, Y. C. Liu, M. H. Chiang, S. Kahlal, J. Y. Saillard, C. Liu, *Angew. Chem. Int. Ed.* **2015**, *54,* 13604-13608; (h) J. Li, J. M. White, R. J. Mulder, G. E. Reid, P. S. Donnelly, R. A. J. O'Hair, *Inorg. Chem.* **2016**, *55,* 9858-9868; (i) A. W. Cook, T.-A. D. Nguyen, W. R. Buratto, G. Wu, T. W. Hayton, *Inorg. Chem.* **2016**, *55,* 12435-12440; (j) P.-K. Liao, C.-S. Fang, A. J. Edwards, S. Kahlal, J.-Y. Saillard, C. W. Liu, *Inorg. Chem.* **2012**, *51*, 6577–6591.

[7] (a) M. S. Bootharaju, R. Dey, L. E. Gevers, M. N. Hedhili, J.-M. Basset, O. M. Bakr, *J. Am. Chem. Soc.* **2016**, *138,* 13770-13773; (b) A. Zavras, G. N. Khairallah, T. U. Connell, J. M. White, A. J. Edwards, P. S. Donnelly, R. A. J. O'Hair, *Angew. Chem. Int. Ed.* **2013**, *52,* 8391-8394; (c) A. Zavras, G. N. Khairallah, T. U. Connell, J. M. White, A. J. Edwards, R. J. Mulder, P. S. Donnelly, R. A. J. O'Hair, *Inorg. Chem.* **2014**, *53*, 7429-7437; (d) A. Zavras, A. Ariafard, G. N. Khairallah, J. M. White, R. J. Mulder, A. J. Canty, R. A. J. O'Hair, *Nanoscale*, **2015**, *7*, 18129-18137.

[8] R. S. Dhayal, W. E. van Zyl, C. Liu, *Acc. Chem. Res.* **2016**, *49,* 86-95.

[9] R. Jin, C. Zeng, M. Zhou, Y. Chen, *Chem. Rev.* **2016**, *116,* 10346-10413.

[10] M. Tsuji, N. Miyamae, S. Lim, K. Kimura, X. Zhang, S. Hikino, M. Nishio, *Cryst. Growth Des.* **2006**, *6,* 1801-1807.

[11] R. S. Dhayal, J. H. Liao, S. Kahlal, X. Wang, Y. C. Liu, M. H. Chiang, W. E. Van Zyl, J. Y. Saillard, C. Liu, *Chem. Eur. J.* **2015**, *21,* 8369-8374.

[12] C. F. Albert, P. C. Healy, J. D. Kildea, C. L. Raston, B. W. Skelton, A. H. White, *Inorg. Chem.* **1989**, *28,* 1300-1306.

[13] P.-K. Liao, K.-G. Liu, C.-S. Fang, C. Liu, J. P. Fackler Jr, Y.-Y. Wu, *Inorg. Chem.* **2011**, *50,* 8410-8417.

[14] H. Dumlich, J. Robertson, S. Reich, *arXiv.org, e-Print Arch., Condens. Matter* **2013***,* 1-25.

[15] J.-H. Liao, R. S. Dhayal, X. Wang, S. Kahlal, J.-Y. Saillard, C.-W. Liu, *Inorg. Chem.* **2014**, *53,* 11140-11145.

[16] T.-A. D. Nguyen, B. R. Goldsmith, H. T. Zaman, G. Wu, B. Peters, T. W. Hayton, *Chem. Eur. J.* **2015**, *21,* 5341-5344.

[17] K. K. Chakrahari, J.-H. Liao, S. Kahlal, Y.-C. Liu, M.-H. Chiang, J.-Y. Saillard, C. W. Liu, *Angew. Chem. Int. Ed.* **2016**, *55,* 14704-14708.

[18] CCDC 1571953 $[Cu_{18}H_{16}\{(Ph_2PCH_2)_2\}_6][BF_4][Cl]$ and CCDC 1572032 $[Cu_{16}H_{14}\{(Ph_2P)_2NH)\}_6][(BF_4)_2]$ contain the supplementary X-ray crystallographic data for this paper. These data can be obtained free of charge from The Cambridge Crystallographic Data Centre via www.ccdc.cam.ac.uk/data_request/cif.

[19] D. M. Ho, R. Bau, *Inorg. Chim. Acta* **1984**, *84,* 213-220.

[20] (a) S. Chen, S. Wang, J. Zhong, Y. Song, J. Zhang, H. Sheng, Y. Pei, M. Zhu, *Angew. Chem. Int. Ed.* **2015**, *54,* 3145-3149; (b) A. Das, C. Liu, H. Y. Byun, K. Nobusada, S. Zhao, N. Rosi, R. Jin, *Angew. Chem. Int. Ed.* **2015**, *54,* 3140-3144.

[21] H. Yoo, J. E. Millstone, S. Li, J.-W. Jang, W. Wei, J. Wu, G. C. Schatz, C. A. Mirkin, *Nano Lett.* **2009**, *9,* 3038-3041.

[22] T. Higaki, C. Liu, C. Zeng, R. Jin, Y. Chen, N. L. Rosi, R. Jin, *Angew. Chem. Int. Ed.* **2016**, *55,* 6694-6697.

[23] Y. Chen, C. Zeng, C. Liu, K. Kirschbaum, C. Gayathri, R. R. Gil, N. L. Rosi, R. Jin, *J. Am. Chem. Soc.* **2015**, *137,* 10076-10079.

[24] (a) Q. Li, S. Wang, K. Kirschbaum, K. J. Lambright, A. Das, R. Jin, *Chem. Commun.* **2016**, *52,* 5194-5197; (b) X.-K. Wan, S.-F. Yuan, Z.-W. Lin, Q.-M. Wang, *Angew. Chem.* **2014**, *126,* 2967-2970.

[25] (a) S. Wang, S. Jin, S. Yang, S. Chen, Y. Song, J. Zhang, M. Zhu, *Sci. Adv.* **2015**, *1, e*1500441-e1500446; (b) A. Das, T. Li, K. Nobusada, C. Zeng, N. L. Rosi, R. Jin, *J. Am. Chem. Soc.* **2013**, *135,* 18264-18267; (c) C. Zeng, Y. Chen, K. Iida, K. Nobusada, K. Kirschbaum, K. J. Lambright, R. Jin, *J. Am. Chem. Soc.* **2016**, *138,* 3950-3953; (d) H. Yang, Y. Wang, A. J. Edwards, J. Yan, N. Zheng, *Chem. Commun.* **2014**, *50,* 14325-14327; (e) C. Zeng, Y. Chen, C. Liu, K. Nobusada, N. L. Rosi, R. Jin, *Science Advances* **2015**, *1,* e1500425; (f) H. Yang, Y. Wang, X. Chen, X. Zhao, L. Gu, H. Huang, J. Yan, C. Xu, G. Li, J. Wu, A.J. Edwards, B. Dittrich, Z. Tang, D. Wang, L. Lehtovaara, H. Häkkinen, N. Zheng, *Nature Commun.* **2016**, *7*, 12809.

[26] C. Liu, T. Li, G. Li, K. Nobusada, C. Zeng, G. Pang, N. L. Rosi, R. Jin, *Angew. Chem. Int. Ed.* **2015**, *54,* 9826-9829.

[27] A reviewer has raised an important question of whether there are hydride ligands located at the center of the Cu16 core. While a neutron diffraction structure would answer this question, the electron density peaks from the X-ray diffraction study are consistent with hydride ligands bound to the Cu surface atoms. For a review with discussions on the encapsulation of hyrides at the centres of coinage metal clusters, see: (a) C. Latouche, C. W. Liu,

J.-Y. Saillard, *J. Cluster Sci.*, **2014**, *25*, 147–171. For a review on the structure and bonding of large molecular ligated metal clusters, see: (b) J.-Y. Saillard, J. F. Halet, *Struct. Bond.*, **2016**, *169*, 157-179.

[28] C. Zeng, Y. Chen, A. Das, R. Jin, *J. Phys. Chem. Lett.* **2015**, *6,* 2976-2986.

[29] Z. Mao, J.-S. Huang, C.-M. Che, N. Zhu, S. K.-Y. Leung, Z.-Y. Zhou, *J. Am. Chem. Soc.* **2005**, *127,* 4562-4563.

[30] M. S. Eberhart, J. R. Norton, A. Zuzek, W. Sattler, S. Ruccolo, *J. Am. Chem. Soc.* **2013**, *135,* 17262-17265.

[31] A. J. Edwards, *Aust. J. Chem.*, **2011**, *64*, 869-872.

[32] P. V. Kishore, J.-H. Liao, H.-N. Hou, Y.-R. Lin and C. Liu, *Inorg. Chem.*, **2016**, 55, 3663-3673.

[33] X. Jia, J. Li, E. Wang, *Small* **2013**, *9,* 3873-3879.

[34] (a) D. J. Lindberg, A. Wenger, E. Sundin, E. Wesén, F. Westerlund, E. K. Esbjörner, *Biochemistry* **2017**, *56,* 2170-2174; (b) Y. Hong, J. W. Lam, B. Z. Tang, *Chem. Soc. Rev.* **2011**, *40,* 5361-5388; (c) P. P. H. Cheng, D. Silvester, G. Wang, G. Kalyuzhny, A. Douglas, R. W. Murray, *J. Phys. Chem. B.* **2006**, *110,* 4637-4644.

[35] Y. Wang, X.-K. Wan, L. Ren, H. Su, G. Li, S. Malola, S. Lin, Z. Tang, H. Häkkinen, B. K. Teo, *J. Am. Chem. Soc.* **2016**, *138,* 3278-3281.

[36] (a) T.-A. D. Nguyen, Z. R. Jones, D. F. Leto, G. Wu, S. L. Scott, T. W. Hayton, *Chem. Mater.* **2016**, *28,* 8385-8390; (b) P. N. Floriano, Noble, J. M. Schoonmaker, E. D. Poliakoff, R. L. McCarley, *J. Am. Chem. Soc.* **2001**, *123,* 10545-10553; (c) C. Ganesamoorthy, J. Weßing, C. Kroll, R. W. Seidel, C. Gemel, R. A. Fischer, *Angew. Chem. Int. Ed.* **2014**, *53,* 7943-7947.

[37] M. A. Huertos, I. Cano, N. A. Bandeira, J. Benet-Buchholz, C. Bo, P. W. van Leeuwen, *Chem. Eur. J.* **2014**, *20,* 16121-16127.

Entry for the Table of Contents (Please choose one layout)

Layout 1:

COMMUNICATION

Copper Hydrides

Frustum-Shaped Ligated nanoclusters: The reduction of Cu(I) precursors yielded the smallest triangular frustum-shaped Cu polyhydrido nanoclusters, $[Cu_{18}H_{16}(DPPE)_6][BF_4][Cl]$ and $[Cu_{16}H_{14}(DPPA)_6][(BF_4)_2]$. The Cu nanoclusters maintained their metal core after the complete hydride loss in the gas phase.

Jiaye Li, Howard Ma, Gavin E. Reid, Alison Edwards, Yuning Hong, Jonathan M. White, Roger J. Mulder and Richard A. J. O'Hair**

Page No. – Page No.

Synthesis and X-ray Cystallographic Characterisation of Frustum-Shaped Ligated $[Cu_{18}H_{16}(DPPE)]^{2+}$ and $[Cu_{16}H_{14}(DPPA)_6]^{2+}$ Nanoclusters and Studies on their H_2 Evolution Reactions

Layout 2:

COMMUNICATION

((Insert TOC Graphic here))

*Author(s), Corresponding Author(s)**

Page No. – Page No.

Title

Text for Table of Contents